The used SFRC mix contains high-strength cold-drawn wire hooked end fibres (DRAMIX RC-80/30-CP) with a length of 30 mm, a diameter of 0.38 mm and a tensile strength of at least 3000 N/mm². This high-performance steel fibre is combined with a concrete strength class of C50/60, while fibre dosage ranged between 20 and 60 kg/m³ (i.e. 0.25-0.75 %) for all SFRC mixes. The mix composition is given in Table 2.

Table 2: SFRC mix composition [kg/m³]

Sand 0/1	202
Sand 0/4	674
Crushed limestone 2/6	257
Crushed limestone 6/14	566
CEM I 52.5 R/HES	390
Fly ash	60
Water	190
Superplasticizer	2.61
RC-80/30-CP	20-60

The production process of the girders is as follows: first, the constituents are loaded in a concrete truck mixer and the concrete is mixed for about 2 minutes. Then, the fibres are added manually to the mix and the additional mixing time is adjusted in order to obtain a good dispersion of all fibres. Additional standard specimens are cast in order to obtain both the cube and cylinder compressive strength and the residual flexural parameters according to the European standard EN-14651 (CEN, 2005).

During testing, the displacements at the point load and at the midspan are monitored by means of linear variable differential transformers (LVDT). The concentrated load is applied by means of a 1000 kN hydraulic jack, placed at a distance of 221 mm and 266 mm from the supports for shear span to depth ratios equal to 2.5 and 3.0 respectively.

2.2 Results and discussion

2.2.1 SFRC properties

For all of the tested girders, the residual flexural stresses $f_{R,i}$ of the SFRC are determined by means of a standard three-point bending test on notched prisms (EN 14651). At defined crack mouth opening displacement (CMOD), the residual stresses are calculated by Eq. 1.

$$f_{R,i} = \frac{3F_{R,i}L}{2bh_{sp}^2} \tag{1}$$

where i=1..4, respectively for CMOD values 0.5, 1.5, 2.5 and 3.5 mm, and $F_{R,i}$ is the applied load at CMOD = i, L the span length (i.e. 500 mm), b the width of the prism and h_{sp} the height of the prism above the notch.

The characteristic residual stress f_{Rk} is calculated based on the average value f_{Rm} and the coefficient of variation δ as follows:

$$f_{Rk} = f_{Rm}(1 - k\delta) \tag{2}$$

where k is a constant value as a function of the number of tests.

The averages values of f_{R1} and f_{R3} and their corresponding characteristic value are summarized in Table 3.

Table 3: SFRC properties

Mix	# tests (k)	V_f [kg/m³]	$f_{R1,m}$ [N/mm²]	c.o.v. [%]	$f_{R1,k}$ [N/mm²]	$f_{R3,m}$ [N/mm²]	c.o.v. [%]	$f_{R3,k}$ [N/mm²]
20A	3 (1.91)	20	2.59	19.7	1.62	4.09	17.2	2.73
20B	6 (1.71)	20	4.88	6.2	4.35	5.91	5.3	5.35
40A	3 (1.91)	40	7.59	15.2	5.45	8.15	17.6	5.41
40B	6 (1.71)	40	6.66	36.5	2.33	7.08	32.9	2.93
60	5 (1.78)	60	10.37	14.4	7.66	9.85	20.7	6.16

Characteristic residual stress values f_{R3k} between 2.73 and 6.16 N/mm² were obtained for SFRC mixes containing 20-60 kg/m³ of fibres. A coefficient of variation around 20 % was found for mixes 20A, 40A, 20/20 and 60. For mix 20B, the observed scatter is much lower, which resulted in a relatively high characteristic value. In contrast, high scatter was observed for mix 40B, which resulted in a significantly lower characteristic value for the residual flexural stresses. For a given concrete mix and fibre type, the ratio between f_{R3k} and the nominal fibre content is inversely proportional to the observed scatter. When the c.o.v. is higher than 25%, the economic use of steel fibres is questionable. This highlights the importance of proper mixing and quality control for production environments.

2.2.2 Shear capacity of prestressed girders

All girders showed similar failure mechanisms. In general, the following stages have been observed:

1) An uncracked linear elastic phase;
2) The occurrence of a diagonal tension (web-shear) crack in the thin web;
3) Additional parallel cracking with increased shear crack propagation;
4) Initiation of bending cracks;
5) Failure of compressive struts / snap-through of flanges.

The experimentally obtained maximum shear strengths of all tested girders are summarised in Table 5.

Table 5: Overview of shear capacities

Girder	F1-2.5	F2-2.5	F3-2.5	F2-3.0
0A	702	647	578	-
0B	-	-	-	536
20A	756	781	609	-
20B	786	-	-	570
40A	799	809	737	-
40B	744	-	-	599
60	672	-	721	627

For an a/d ratio equal to 3.0, the observed shear capacity of the prestressed girders is lower than for a/d = 2.5. This can be explained as follows: for lower shear span to depth ratios, the applied load is transmitted directly to the supports and an arch action settles in leading to higher shear loads, while for higher a/d-ratios, a girder action failure type is more likely to occur which results into a reduction of shear capacity.

In case of a/d equal to 2.5, further differences are found between the shear capacities as a function of test phase. In general, the shear critical area is always near the end-blocks and phase 1 and 2 will be more representative of realistic situations. However, it is found that when shear failure occurs in the absence of a rigid end-block, it is easier for the shear critical area to deform and a significant decrease of shear capacity is observed for girders 0A, 20A and 40A when the shear test is carried out in phase 3.

In Figure 4, the observed shear capacity of the tested girders is plotted as a function of the characteristic residual flexural stress f_{R3k}. For a/d equal to 2.5 and for the same testing phase, the maximum shear load increases for f_{R3k} up to about 5.5 N/mm². For girder test 60-F1 and 60-F3 (with highest values of f_{R3k}), the shear capacity does not follow the increasing trend, which indicates a limitation of the beneficial effect of the fibres as shear reinforcement. For the relationship between V_{exp} and f_{R3k} in case of a/d = 3.0, an increasing trend is observed for the complete f_{R3k} test range.

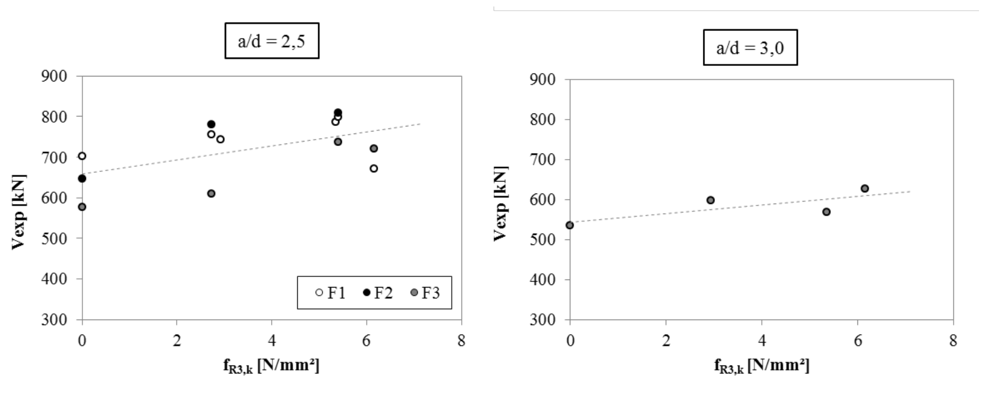

Figure 3: Experimentally observed shear capacity as a function of f_{R3k} for a/d = 2.5 (left) and a/d = 3.0 (right).

3 Verification of design models

In Model Code 2010, two fundamentally different design approaches are presented. The first model is mainly an adaptation of the shear design equation for plain concrete. It is assumed (Minelli, 2005; Minelli, 2013) that fibres enhance the aggregate interlock mechanism and hence, the beneficial effects of fibres is taken into account by increasing the longitudinal reinforcement ratio with a factor that includes the post-cracking tensile strength of fibre-reinforced concrete. In order to verify the experimentally observed shear capacities, all safety factors are taken equal to one and the average material properties are used. The shear resistance of prestressed concrete members without conventional reinforcement is then given by:

$$V_{Rm,F1} = \left(0.18 \cdot k \cdot \left[100 \cdot \rho_l \left(1 + 7.5 \cdot \frac{f_{Ftum}}{f_{ctm}}\right) \cdot f_{cm}\right]^{1/3} + 0.15 \cdot \sigma_{cp}\right) \cdot b_w \cdot d \tag{5}$$

where

k	size effect factor $= 1 + \sqrt{\frac{200}{d}} \leq 2$	[-]
d	effective depth of the cross section	[mm]
ρ_l	longitudinal geometrical reinforcement ratio $= \frac{A_{sl}}{b_w d}$	[-]
f_{cm}	average cylinder compressive strength	[N/mm²]
f_{Ftum}	average value of the ultimate residual tensile strength	[N/mm²]
f_{ctm}	average tensile strength of the concrete	[N/mm²]
σ_{cp}	average stress acting on the cross section due to prestress	[N/mm²]
b_w	smallest width of the cross section in the tensile area	[mm]

Although this model is validated with respect to other experimental data, it is not in accordance with the general shear design approach for RC structures. Therefore, a second design approach is presented in the MC2010 commentary section, which is in line with the shear design of Level III of Approximation (LoAIII), based on the Modified Compression Field Theory (MCFT) for traditionally reinforced concrete (Vecchio, 1986). The shear resistance can be calculated as follows:

$$V_{Rm,F2} = \left(k_v \sqrt{f_{cm}} + f_{Ftum} \cot\theta\right) \cdot b_w \cdot z \tag{6}$$

The first term between the brackets is counting for the concrete contribution as a result of aggregate interlocking in which the strain effect factor k_v (Bentz, 2006) is given by:

$$k_v = \frac{0.4}{1 + 1500\varepsilon_x} \tag{7}$$

The inclination of the compression strut is calculated by means of eq. 8.

$$\theta = 29° + 7000\varepsilon_x \tag{8}$$

Both equations 7 and 8 require the strain ε_x calculated at the cross section mid-depth. Since the value of ε_x depends on the maximum shear force $V_{Rm,F2,}$ the set of equations 6 to 9 is to be solved iteratively.

$$\varepsilon_x = \frac{\frac{M_i}{z} + 0.5\cot\theta \cdot V_{Rm,F2_i} - A_p f_{p0}}{2(E_s A_s + E_p A_p + E_c A_c)} \geq -0.002 \tag{9}$$

where

M_i	flexural moment in the middle of the shear span (i^{th} iteration)	(Nmm)
$V_{Rm,F2i}$	calculated shear capacity (i^{th} iteration)	(N)
E	modulus of elasticity *	(N/mm²)
A	cross section *	(mm²)
f_{p0}	initial prestress	(N/mm²)
z	internal lever arm (= 0.9 d)	(mm)

* the indices s, p and c stand for steel, prestress strand and concrete respectively.

The value of f_{Ftum}, is calculated based on the bi-linear model (*fib*, 2010) for SFRC according to equations 10 and 11 by assuming w_u equal to 1.5 mm. All calculated values are reported in Table 6.

$$f_{Ftum} = f_{Fts} - \frac{w_u}{2.5}(f_{Ftsm} - 0.5 f_{R3m} + 0.2 f_{R1m}) \tag{10}$$

$$f_{Ftsm} = 0.45 f_{R1m} \tag{11}$$

Table 6: Calculated values defining the linear post-cracking constitutive law for SFRC

Girder	f_{Ftsm} [N/mm²]	f_{Ftum} [N/mm²]
20A	1.17	1.38
20B	2.20	2.07
40A	3.42	2.90
40B	3.00	2.52
60	4.67	3.58

The ratio between experimental (V_{exp}) and calculated shear load (V_{cal}) is shown in Figure 5. For each design model, the average value (avg.) and the coefficient of variation (c.o.v.) of the ratio V_{exp}/V_{cal} is mentioned.

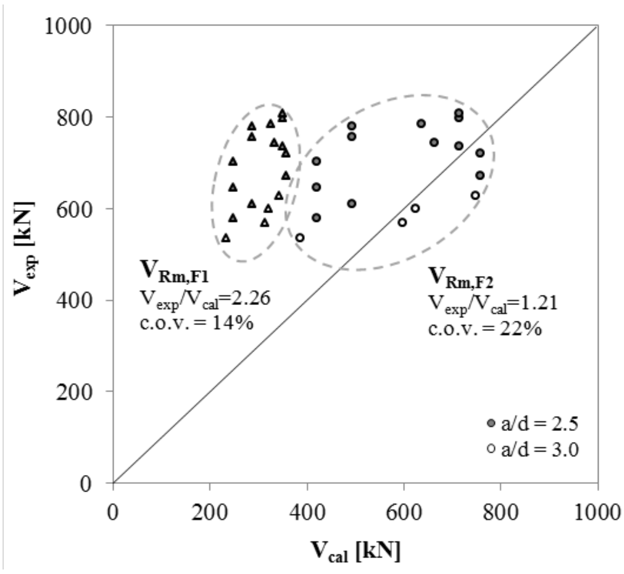

Figure 5: Comparison between experimental and calculated shear capacity for $V_{Rm,F1}$ and $V_{Rm,F2}$.

It can be seen in Figure 5 that Eq. 5 ($V_{Rm,F1}$) yields very conservative values compared to the alternative model $V_{Rm,F2}$ (Eqs. 6-9). Although the latter model is more accurate to predict the experimentally observed shear capacity, a higher model uncertainty is observed.

4 Conclusions

Based on 17 shear tests on prestressed concrete girders without shear reinforcement and with steel fibres (0.25-0.75 %), it can be concluded that steel fibres can increase the shear strength of full-scale girders and can be used to replace the minimum required traditional reinforcement according to Model Code 2010.

A limitation of the beneficial effect of fibres to increase shear strength is found for girders tested with a shear-span to depth ratio equal to 2.5 (phase 1 and 2) for a value of f_{R3k} around 5 N/mm². Although this limitation is not found for girders tested with an a/d ratio equal to 3.0, the observed increase of shear strength as a function of residual tensile strength is lower than for a/d = 2.5.

When the design models for shear proposed in Model Code 2010 are used to predict the experimentally observed capacity, it is found that both provisions yield different accuracy with $V_{Rm,F1}$ being very conservative. Although the calculation procedure based on the Modified Compression Field Theory (MCFT) is more elaborate, it has a more physical descriptive background and can lead to a more economical design of pretensioned precast concrete girders where stirrups are completely replaced by steel fibres.

5 Acknowledgements

The authors would like to express their utmost gratitude to the Agency for Innovation through Science and Technology (IWT) and the companies Megaton, member of the Willy Naessens Group, and Bekaert for providing financial and technological support, respectively.

6 References

Bentz, E.C.; Vecchio, F.J.; Collins, M.P. (2006), Simplified Modified Compression Field Theory for Calculating Shear Strength of Reinforced Concrete Elements. *ACI Structural Journal*, Vol. 103, No. 4, pp. 614-624.

Cuenca, E.; Serna, P. (2013), Shear behavior of prestressed precast beams made of self-compacting fiber reinforced concrete. *Construction and Building Materials*, Vol. 45, pp. 145–156.

EN 14651:2005 - *Test method for metallic fibered concrete - measuring the flexural tensile strength*.

Fédération internationale du béton (*fib*). (2013) *fib Model Code for Concrete Structures 2010.* Ernst & Sohn, Berlin, Germany.

Meda, A.; Minelli, F.; Plizzari, G.A.; Riva, P. (2005), Shear behaviour of steel fibre reinforced concrete beams. *Materials and Structures*, Vol. 38, pp. 343-351.

Minelli, F. (2005), *Plain and Fibre Reinforced Concrete Beams under Shear Loading: Structural Behaviour and Design Aspects*. University of Brescia, Brescia, Italy.

Minelli, F.; Plizzari, G.A. (2013), On the Effectiveness of Steel Fibres as Shear Reinforcement. *ACI Structural Journal*, Vol. 110, No. 3, pp. 379-389.

Parra-Montesinos, G.J. (2006), Shear strength of beams with deformed steel fibers. *Concrete International*, Vol. 28, No. 11, pp. 57-61.

Soetens, T.; Matthys, S. (2013), *Evaluation of MC2010 models for prestressed SFRC beams subjected to shear*. 7th International Conference: Fibre Concrete 2013: Technology, Design, Application, A. Kohoutkova (Ed.), Prague, Czech Republic.

Vecchio, F.J.; Collins, M.P. (1986), The Modified Compression-Field Theory for Reinforced Concrete Elements Subjected to Shear. *ACI Journal*, Vol. 83, No. 22, pp. 219-231.

Numerical modelling of large scale steel-fibre-reinforced reinforced concrete beams failing in shear

Ali Amin, Stephen J. Foster

University of New South Wales, Sydney, Australia

Abstract

Experimental and numerical studies on steel-fibre-reinforced concrete (SFRC) over the last five decades, or so, have indicated that the post cracking strength of concrete can be improved by providing suitably arranged, closely spaced, wire reinforcement. While the database of experimental and numerical shear tests of SFRC members is extensive, the pool of test data and numerical models, alike, of SFRC beams containing conventional transverse shear reinforcement (stirrups) are limited. The behaviour of full scale steel-fibre-reinforced reinforced concrete (SFR-RC) beams are analysed herein using a smeared crack model provided by ATENA 2D integrated with a constitutive law derived after an inverse analysis from prism bending tests. The numerical model is validated against experimental results obtained from four large scale SFR-RC beams and is shown to reasonably model the experimental responses. The model allows a better understanding of SFR-RC structures failing in shear and can be used as a basis for developing new design procedures for such structures.

Keywords

Steel fibres, concrete, shear, stirrups, ATENA.

1 Introduction

Experimental and numerical investigations have shown that the inclusion of steel fibres in concrete, when adopted in adequate quantities, can improve the shear resistance of beams by increasing the post cracking strength of the concrete. Fibres embedded within concrete delay the propagation and growth of cracks by improving the effectiveness of the crack-arresting mechanisms present when beams are subjected to high shear stresses.

Many studies have considered the possibility of utilizing SFRC by assigning a proportion of the shear resisting capacity of beams to the fibres. This has been realized by ACI-318 (2008), and more recently by the *fib* Model Code 2010 (2012) and the Draft Australian Bridge Code: Concrete (2014). Some inconsistencies in some of these approaches, however, have been identified (Foster, 2010; Amin & Foster, 2014).

To accurately model the inherent nonlinear properties of elements composed of SFRC, it is necessary to make use of advanced software which can correctly model concrete fracture. This is of particular importance when crack propagation at the elemental level can significantly influence the global, or structural, response of the member (Foster & Voo, 2004, Foster et al., 2006, Minelli & Vecchio, 2006). To this end, a numerical investigation is undertaken to study, in detail, the development of shear resistant mechanisms in steel-fibre-reinforced reinforced concrete beams with and without conventional shear reinforcement using a commercially available Finite Element package, ATENA 2D, developed by Cervenka Consulting (Cervenka et al., 2002).

The numerical model is validated against experimental results obtained from four 5 metre long by 0.3 metre wide by 0.7 metre high rectangular simply supported beams with varying transverse and fibre reinforcement ratios. An evaluation of the transverse stirrup contribution versus fibre contribution to the shear capacity is compiled and recommendations are made for the explicit inclusion of the distinct capacities to existing design models.

2 Experimental investigation

An experimental program was conducted to investigate the combined effect of steel fibres and traditional transverse reinforcement on the response of large scale beams subjected to four-point loading. Four beams with various fibre and transverse reinforcement ratios were constructed and tested to failure. As the investigation was designed for the specimens to fail in shear, the beams were designed to ensure that flexural tensile failure did not occur.

The specimen dimensions and testing arrangements are shown in Figure 1. The specimens are designated using the notation BX-Y-Z where 'X' is the dosage of fibres (in kg/m^3), 'Y' is the diameter of stirrup (in mm), and 'Z' is the stirrup spacing (in mm) within the critical shear regions. For example, specimen B25-10-450 represents a beam reinforced with 25kg/m^3 of steel fibres and 10mm stirrups spaced at 450 mm c/c.

The longitudinal reinforcement was fabricated from nominally 500 MPa grade, hot rolled, deformed bars. The beams contained two layers of three normal ductility 28 mm diameter tensile reinforcement (N28), which corresponds to a flexural reinforcement ratio of 1.98%. Two 20 mm diameter longitudinal reinforcing bars (N20) were located at the top section of the beam. The measured yield strength of the longitudinal bars was 540 MPa. The 2-leg stirrups were fabricated from hard-drawn wire reinforcement and were spaced at 450 mm centres. The 10 mm diameter stirrups had a yield strength of 450 MPa; the 6 mm stirrups had a yield strength of 550 MPa. The steel fibres used in this study were the double end-hooked Dramix®5D-65/60-BG fibre. The fibres were 0.9 mm in diameter and 60 mm long. The specimens were cast using a single batch of concrete obtained from a local ready mix supplier. The concrete had a prescribed characteristic compressive strength of 32 MPa and the aggregate used was basalt with a maximum particle size of 10 mm. All beam specimens were tested in an Instron 5000 kN stiff testing frame and tested under a ram displacement control of 0.3mm/min. A linear strain conversion transducer (LSCT) was placed at the beam mid-span to measure displacement (Figure 1). The reader is referred to Amin and Foster (2014) for further details on the experimental study.

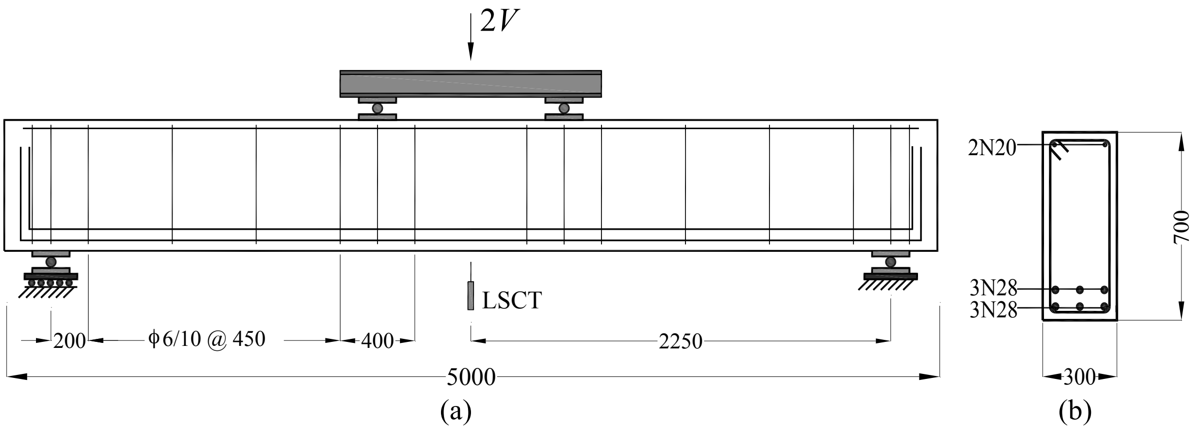

Figure 1: Specimen dimensions (in mm): (a) Test setup; (b) Cross section.

3 Mechanical properties of SFRC

The measured mechanical properties of the SFRC at the time of testing are presented in Table 1. The fracture properties of SFRC were determined directly by obtaining the tensile strength of the concrete matrix, f_{ct}, and the residual tensile strength, $f_{1.5}$ (taken at a crack width of 1.5mm), from six uniaxial 'dogbone' specimens tested to DR AS5100.5 (2014). The tensile properties were also determined indirectly from the residual flexural strength, $f_{R,j}$, through five three-point notched prisms tested to EN 14651 (2007). The mean compressive strength (f_{cm}) and Young's modulus (E_c) were determined by testing three 150 mm diameter x 300 mm cylinders.

Table 1: Mechanical properties of SFRC

f_{cm} (MPa)	E_c (GPa)	f_{ct} (MPa)	$f_{1.5}$(MPa)	f_{R1} (MPa)	f_{R2} (MPa)	f_{R3} (MPa)	f_{R4} (MPa)
34	28	2.45	0.68	2.39	2.52	2.56	2.26

To define the tensile stress versus crack opening displacement fracture constitutive relationship for SFRC, the simplified inverse analysis procedure developed by Amin et al. (2013) was used in this study. The formulation of this model is founded upon a sectional analysis of a prism in bending and considers the influence of fibres on the moment carried by the specimen from the point in the test where the un-cracked concrete has little influence on the prism capacity and considers rigid body rotations. The nominal stress carried by the fibres, $f(w)$, is taken as:

$$f(w) = k_b\left(\frac{f_{R2}}{3} + (f_{R4} - f_{R2})\xi(w)\right) \geq 0 \tag{1a}$$